Study on Construction Optimization Method of Tunnel Crossing Fault Fracture Zone

Jiahui Wang[1], Chunyang Dou[1], Xing Li[1], Jian Che[1], Shuang Zhang[2], Ruiyao Wang[1], Yi Zhu[1], Shiji Sun[1], Zhen Liu[3], Tong Wu[1]*

[1] School of Civil Engineering, Heilongjiang University, 74 Xuefu Road, Nangang District, 150080 Harbin, China
[2] Liaoning Provincial Transportation Planning & Design Institute Co., Ltd., 42 Lidao Road, Heping District, 110166 Shenyang, China
[3] Longjian Road and Bridge Company Limited, 109 Songshan Road, Nangang District, 150090 Harbin, China
* Corresponding author, e-mail: ldwutong@hlju.edu.cn

Abstract

When a highway tunnel intersects a fault fracture zone, the excavation process disrupts the surrounding weak and fragmented rock mass, compromising the stability of the fault zone. This study compares the deformation and stress distribution of the surrounding rock using the reserved core soil method, central diaphragm (CD) method, and cross diaphragm (CRD) method during tunnel excavation through fault fracture zones. Among these, the CRD method is identified as the safest construction technique. Additionally, to address the significant deformation of the surrounding rock when tunneling through fault zones, the impact of various pre-support and advance reinforcement techniques on rock mass deformation is analyzed. By comparing the full-ring grouting method with the optimized reinforcement zone approach, the findings demonstrate that optimized grouting significantly reduces disturbance to the fault fracture zone during excavation, thereby enhancing the overall stability of the surrounding rock mass.

Keywords

fault zone, fracture zone, excavation method, numerical simulation, grouting reinforcement

1 Introduction

In tunnel construction, it is often unavoidable to encounter areas with complex geological conditions. When passing through such regions, particularly fault fracture zones, the influence of adverse geological conditions on the tunnel must be carefully considered. Fault fracture zones are characterized by their inherent instability, and factors such as incomplete geological investigation prior to construction and the unpredictable nature of the rock mass can lead to significant deformation of the surrounding rock during excavation. If not properly managed, these challenges pose considerable safety risks to construction personnel. Therefore, it is critical to adopt a scientifically sound construction approach that minimizes deformation of the surrounding rock and ensures the overall stability of the tunnel. The key challenges lie in selecting appropriate excavation techniques, implementing effective pre-support measures, and optimizing construction parameters to mitigate risks associated with the fault fracture zone and achieve safe, stable, and efficient tunnel construction.

The surrounding rock condition of the fault fracture zone is a key factor to be paid attention to during excavation, especially the length, shape and quality of the fault. Huo et al. [1] put forward a new type of NPR anchor cable-truss active-passive coupling bracing system is introduced. The effectiveness of the system in reducing major deformation and damage at the initial branches of the tunnel in the fault fracture zone is evaluated. Jiang et al. [2] and Guo et al. [3] it is pointed out that accurate geological model and considering geological uncertainty are very important to the construction safety of tunnel through fault fracture zone, and affect the application of reinforcement technology such as pre-grouting. Liu et al. [4] and Tang et al. [5] all emphasized the importance of numerical simulation technology in tunnel engineering research. Through numerical simulation, the formation response and surrounding rock deformation can be predicted more accurately when the tunnel passes through the fault fracture zone, which provides a scientific basis

for the optimization of engineering design and construction scheme. At the same time, the numerical simulation technology can greatly reduce the research cost and time cost, and improve the research efficiency. Chen et al. [6] points out that the main reason why the stability of the surrounding rock in the fault fracture zone decreases after tunnel excavation is the erosion of the surrounding rock cracks caused by water seepage.

The application of grouting technology, the proposal of compensation excavation method and the numerical simulation analysis of reinforcement effect are presented to show the importance and diversity of reinforcement and support technology when the tunnel passes through the fault fracture zone. These technologies not only help to improve the stability of tunnel excavation face, but also effectively reduce deformation and damage to ensure the safety and smooth progress of tunnel construction [7–9]. Xu et al. [10] explains the influence of inclination Angle on tunnel structural damage. In the process of tunnel excavation, how many factors such as geological structure, tunnel spacing, fault Angle and construction steps interact together affect the stability and safety of surrounding rock and existing structures [11-13] Xue et al. [14] discussed the impact of different construction schemes on the safety of undersea tunnel crossing the fracture zone in a comprehensive way. Li et al. [15] used the material point method (MPM) to simulate the failure response of rock tunnel surfaces during excavation in fault fracture zones.

Although existing studies have extensively investigated the excavation process of surrounding rock in fault fracture zones, research on optimized construction measures specifically for fault fracture zones remains limited. Efficient and safe crossing of fault fracture zones continues to be a significant challenge in highway tunnel construction.

This study, based on practical engineering, uses a highway tunnel in Northeast China as the research background. By comparing the deformation and stress distribution of surrounding rock during tunnel excavation using the reserved core soil method, central diaphragm (CD) method, and cross diaphragm (CRD) method, the most optimal and safe excavation method is identified. Furthermore, to address the issue of significant surrounding rock deformation when tunnels pass through fault fracture zones, pre-reinforcement measures involving a grouting reinforcement ring and extended reinforcement range were implemented. By comparing the ring grouting method with the reinforcement range optimization method, the effects of optimized grouting measures

on deformation and stress in the fault fracture zone during excavation are analyzed.

2 Project overview and model establishment
2.1 Project overview
The length of a special tunnel in Northeast China is 4400 m, the design speed is 80 km/h, the construction net height is 5.00 m, the net width is 10.25 m. In the process of excavation of this project, a fault fracture zone appeared, and the rock mass was relatively broken. The surrounding rock in this fault area was rated as grade V, with grade IV surrounding rock on both sides of the fault, the fault length was 200 m, and the fault inclination was 87°. The average maximum buried depth at the fault was 320 m, as shown in Fig. 1.

According to the design specifications, the tunnel crossing the fault fracture zone is excavated using the CD method. During excavation, pre-support measures or Advance Support with Small-Diameter Pipes must be implemented. The thickness of the initial support is set at 0.2 m, and enhanced protection is applied following the V_2-class composite lining standards.

2.2 Material parameters
In the process of tunnel construction, the properties of materials directly affect the selection of construction methods and the stability and safety in the construction process. The physical and mechanical properties of rock, shotcrete and other materials, such as elastic modulus and compressive strength, are key factors that need to be accurately considered in design and construction. In this section, some of the main material parameters affecting tunnel construction will be described in detail:

1. Rock structure:
   Rock exhibits unique distribution and strength characteristics, with significant influences from
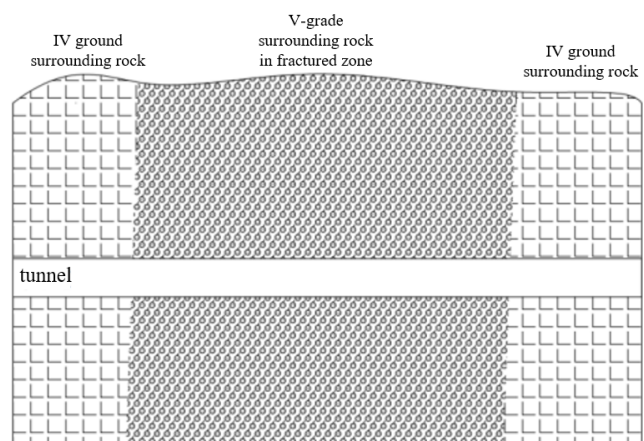

Fig. 1 Schematic diagram of fault fracture zone

principal stresses. The effects of compressive and tensile stresses on rock behavior differ considerably. The Mohr-Coulomb strength criterion is currently widely applied in rock mechanics calculations. This criterion considers the maximum shear stress or the singular shear stress under normal stress or mean stress, based on shear failure theories. According to this criterion, the primary failure mode of rock masses is shear-induced fracturing.

Rocks possess cohesion, frictional coefficients, and internal friction angles. When the shear stress within the rock reaches or exceeds the combined value of its cohesion, frictional coefficient, and internal friction angle, the rock mass reaches its ultimate state, leading to yielding and failure.

The expression is: $\tau = c + \sigma \tan\varphi$, where the formula of friction force is $f = \sigma \tan\varphi$ is the shear strength, c is the cohesion force, σ is the normal stress, φ is the internal friction angle, so the yield failure of rock is related to the magnitude of shear stress and normal stress, as shown in Fig. 2.

As shown in Fig. 2, the tangent point between the shear strength curve and the Mohr stress circle signifies the limit equilibrium state. When the shear curve is disjoint from the stress circle, the stress at that point remains within the safe threshold, not reaching the critical limit. Conversely, when the shear curve intersects the stress circle, the stress at the intersection exceeds the tolerable limit.

2. Elastic modulus of shotcrete:
Equation (1) is used to convert the steel frame into the elastic modulus of shotcrete by using the equivalent stiffness method:

$$E = \frac{E_g \times S_g + E_c \times S_c}{S_{g+c}},\tag{1}$$

where:
- E: equivalent elastic modulus;
- E_g: elastic modulus of I-steel;

Fig. 2 Stress circle and shear strength curve

- E_c: elastic modulus of shotcrete;
- S_g: cross-section area of I-beam;
- S_c: shotcrete cross section area;
- S_{g+c}: shotcrete and I-steel composite cross section area.

3. Equivalent elastic modulus of surrounding rock in the reinforcement area:
Equation (2) was used to calculate the equivalent elastic modulus of surrounding rock in the grouting reinforcement area:

$$E_2 = \rho E_g + (1 - \rho) E_w,\tag{2}$$

where:
- E_2: equivalent elastic modulus of grouting reinforcement area;
- $\rho = (0.6\sim0.7)\eta$, η indicates the porosity of surrounding rock;
- E_g: elastic modulus of the slurry during solidification;
- E_w: elastic modulus of rock mass to be reinforced.

The tunnel involves the initial support, secondary lining and grouting reinforcement area, and the material parameters of surrounding rock and supporting structure should be selected according to the actual geological conditions. The initial support and secondary lining are simulated by combining C30 concrete and steel arch, and the concrete material is elastic material.

In this paper, reference is made to the code for design of highway tunnel [16], code for design of railway tunnel [17], and standard for classification of engineering rock mass [18], in which the division of tunnel surrounding rock and the scope of materials at all levels are specified, and material parameters are reasonably selected. The material parameters of this study are shown in Table 1.

2.3 Finite element modeling
During tunnel excavation, the excavation of rock mass is relatively small compared to the overall model. In order to accurately reflect the influence of excavation on the surrounding rock mass, the grid encryption area is set during grid division. The surrounding rock outside the encrypted area is divided by a larger grid. In this paper, solid 45 units are used to simulate surrounding rock, secondary lining and grouting reinforcement area, and shell surface units are used to simulate steel support and initial support [19]. A grid of 0.5 × 0.5 × 0.5 is used to divide the encryption area, and a grid of 2 × 2 × 1.5 is used for other parts, as shown in Fig. 3.

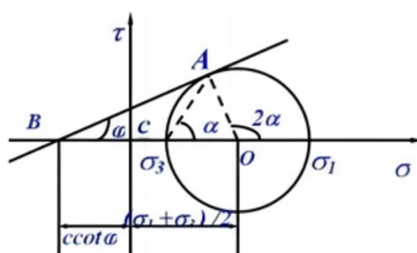Table 1 Parameters of tunnel modeling materials

Soil type	Natural weight (γ) (kN/m^3)	Modulus of elasticity (E) (GPa)	Poisson's ratio (μ)	Angle of internal friction (ϕ) (°)	Cohesion force (c) (MPa)
V-grade crushing zone surrounding rock	18	1	0.4	17	0.08
Crushing zone surrounding rock advance small pipe reinforcement area	18.5	1.5	0.37	20	0.16
Class IV surrounding rock	23	5	0.31	35	0.5
Primary support	24.5	33	0.2	–	–
Secondary lining	24	31.5	0.2	–	–
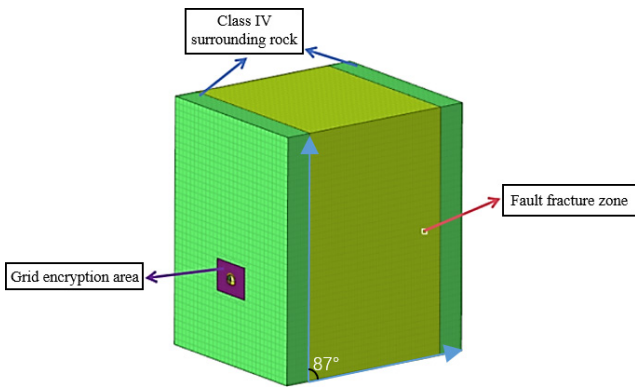
Fig. 3 Model stereogram

Contact unit processing:
- When simulating the contact surface between fault and non-fault, the contact unit is used to reflect the actual situation of surrounding rock more truly. This distinction helps to optimize the accuracy and efficiency of the simulation. The cohesion force and friction Angle of the contact surface unit can be taken up or down 0.5 times of the surrounding rock parameters according to relevant experience [20].
- Fault contact interface method phase stiffness, tangential stiffness and cohesion force can be calculated according to the following equation [21]:

$$K_n = E_i/d_v,\tag{3}$$

$$K_t = G_i/d_v,\tag{4}$$

$$G_i = RG_{soil},\tag{5}$$

$$G_{soil} = \frac{E}{2(1+V_{soil})},\tag{6}$$

where:
- G_i: interface shear modulus;
- G_{soil}: shear modulus of soil and soil;
- V_{soil}: is Poisson's ratio;
- E_i: interfacial elastic modulus;

- d_v: virtual thickness coefficient, generally 0.1;
- R: strength reduction factor, generally 0.3.

3 Simulation study of different excavation methods

Through the simulation of the process of the core earth reservation method, CD method and CRD method passing through the fault fracture zone, the displacement and deformation of the fault fracture zone and the stress distribution of the tunnel supporting structure during the excavation process are analyzed, and the influence of different excavation methods on the stability of surrounding rock is explored.

The CD method is a construction method in which one side of the tunnel is first excavated in a large-span tunnel with weak surrounding rock, and a central diaphragm is constructed, and then the other side is excavated. By dividing the tunnel into two parts, the disturbance range of the surrounding rock is reduced, and the stability of the tunnel is improved.

CRD method is to excavate one or two parts on one side of the tunnel, apply the middle septum and the transverse partition, and then excavate one or two parts on the other side of the tunnel to complete the construction of the transverse partition. Then excavate the last part of the first construction side, and extend the construction method of the middle next door, and finally excavate the remaining part. This method can effectively control the deformation and settlement of surrounding rock by dividing large section tunnel into several small sections for partial excavation and support.

As shown in the Fig. 4, the three drawings respectively represent the excavation schematics of CD method, CRD method and reserved core soil method.
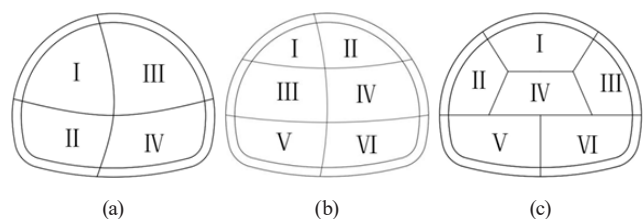

Fig. 4 Diagram of different excavation methods; (a) CD method; (b) CRD method; (c) Core land reservation method

As shown in the Fig. 5, we added the diorama diagram in order to observe the key points of the tunnel more directly.

The monitoring and analysis of surrounding rock deformation and supporting structure stress distribution are helpful to evaluate the influence of different excavation methods on surrounding rock, and provide an important basis for the optimization of construction methods:

1. Displacement and deformation of surrounding rock

   In the process of simulated tunnel excavation, the excavation is carried out step by step along the Z axis from the origin of coordinates. In the process of excavation, it is found that the surrounding rock has obvious deformation near the contact plane between the fault and the IV grade surrounding rock, and the most significant deformation is the central section of the fault, as shown in Figs. 6 to 8.

   As shown in Fig. 6, the displacement of surrounding rock at each monitoring point changes in a similar trend during excavation with different excavation methods, and the displacement curves of each monitoring point change greatly near the fault contact section and then tend to be flat. In the central area of the fault, the displacement of each monitoring point reaches its maximum value.

   According to Fig. 7 before tunnel excavation reaches the central fault section, the displacement change curve of each monitoring point on the central fault section presents a slow growth trend. When the
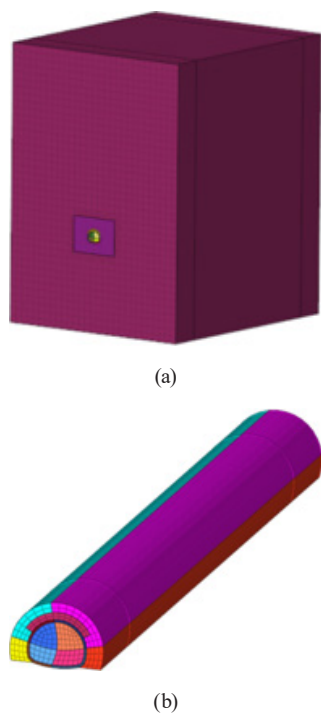

(a)

(b)

Fig. 5 Model stereogram; (a) Model stereogram; (b) Model excavation diagram
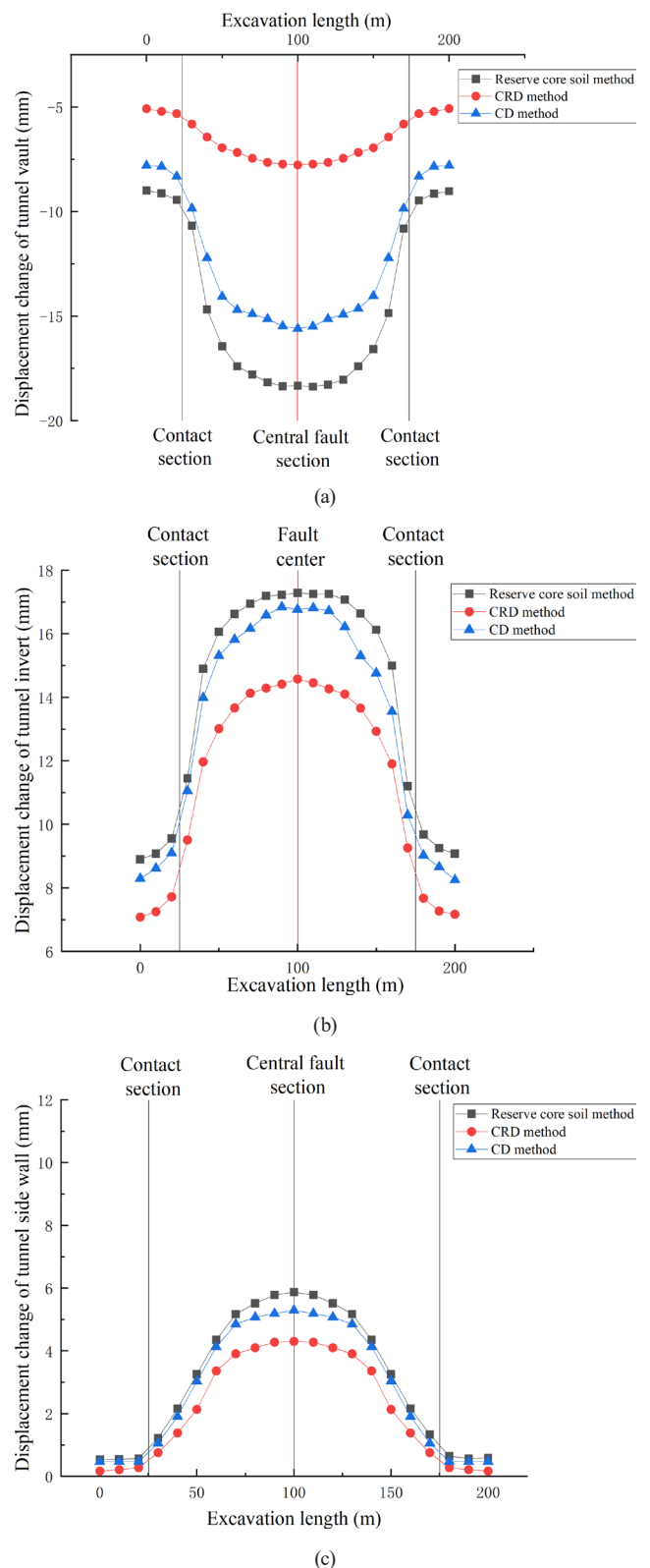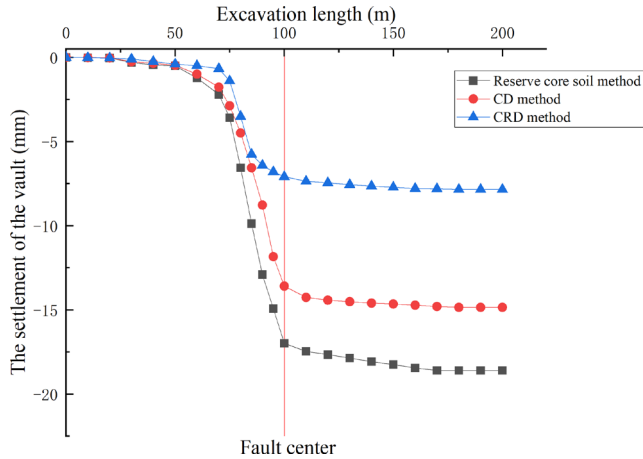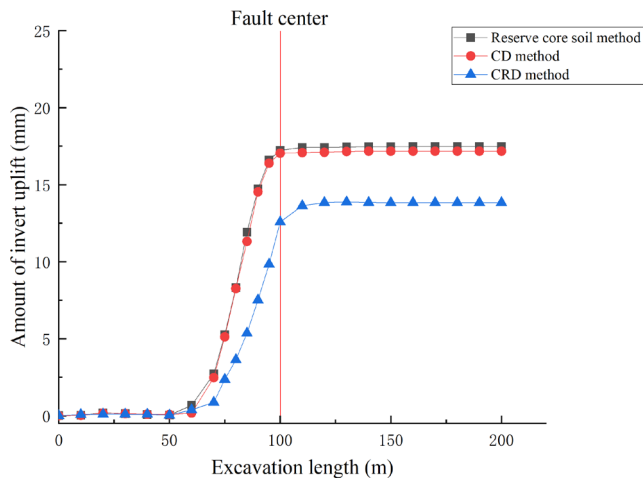

(a)

(b)

(c)

Fig. 6 The final displacement curve of the key points of the fracture zone along the excavation direction; (a) Vault; (b) Invert; (c) Side walls

excavation was about 75 m, the displacement curve of the side wall of the central section of the fault suddenly changed, and the displacement change of the monitoring point began to increase significantly.
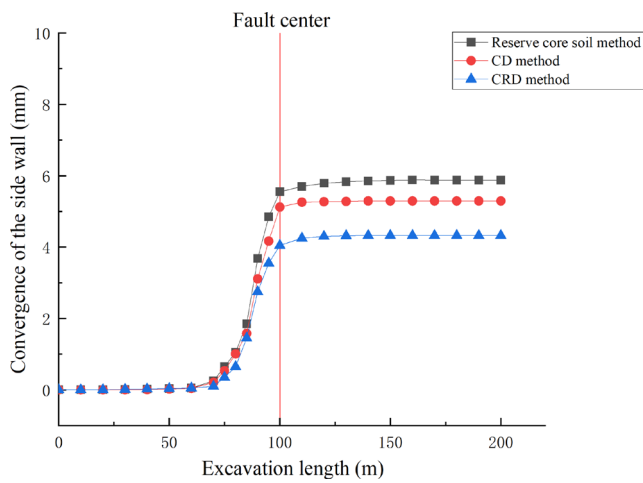
With the completion of section excavation, the initial support of the tunnel forms a closed loop, and the displacement curve of each monitoring point tends to be flat and no longer increases significantly.
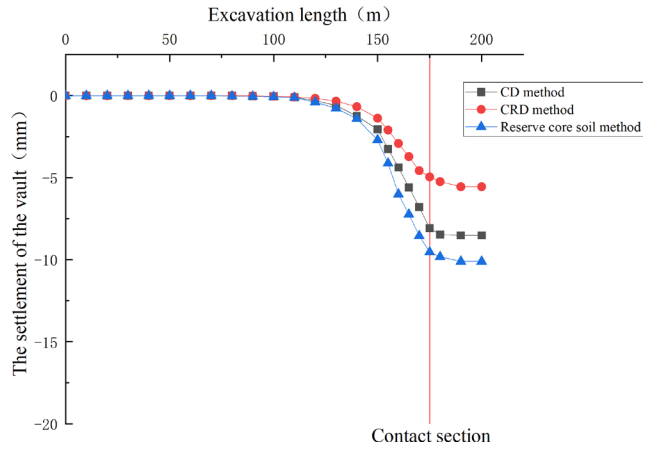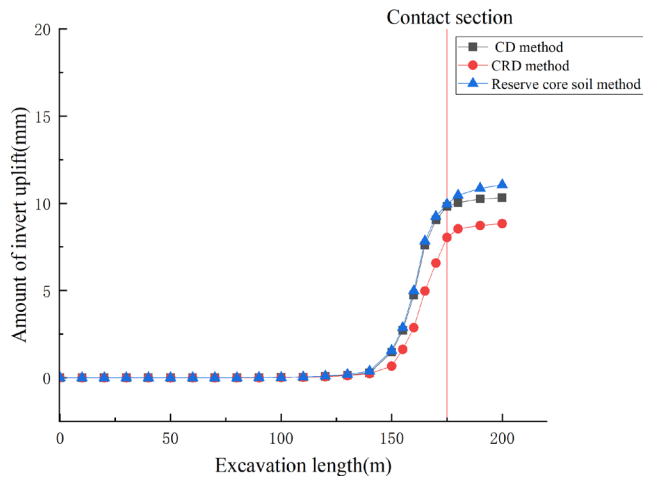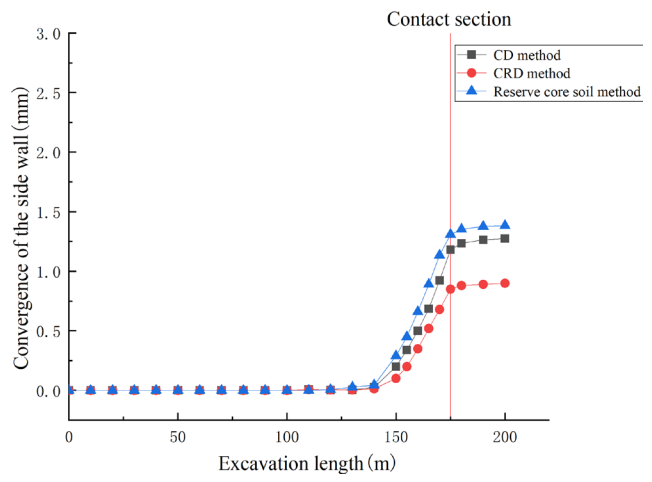
As shown in Fig. 8 at the position of the contact section between the fault and the non-fault the displacement change law of each monitoring point in different sections is similar. During the excavation

(a)

(b)

(c)

Fig. 7 The displacement curve of key points in the central section of fault with excavation; (a) Vault; (b) Invert; (c) Side walls

(a)

(b)

(c)

Fig. 8 Displacement curves of each key point at the contact section with excavation; (a) Vault; (b) Invert; (c) Side walls

with CRD method, the displacement change of each monitoring point is the smallest, because during the excavation with CRD method, the section is divided into 6 parts for excavation, and the middle partition is applied at the same time, thus reducing the disturbance effect on surrounding rock.

Among the three construction methods, CRD method produces the smallest displacement change at each monitoring point during excavation, followed by CD method, and reserved core soil method is the largest.

2. Stress distribution of supporting structure

By comparing the stress distribution of the excavation support structure with the reserved core soil method, CD method and CRD method, the reason is that the existence of the middle septum affects the stress of the tunnel lining structure during excavation. Table 2 shows the stress distribution.

According to Table 2, the maximum principal stress generated by different excavation methods is CD method > reserved core soil method > CRD method, and the minimum principal stress generated is CD method > reserved core soil method > CRD method. According to the code for design of highway tunnels [16], the ultimate tensile strength $R = 2.0$ MPa and the ultimate compressive strength of C25 concrete is 25 MPa according to the damage stage method, the maximum tensile stress and maximum compressive stress of the tunnel supporting structure are both within the safe range.

4 Optimization of grouting reinforcement

In this tunnel, a top grouting reinforcement method is applied in the fault fracture zone. The reinforcement range covers 120 degrees, with a grouting thickness of 1.5 m, using cement mortar as the grouting material. This study proposes the use of the ring grouting method and the reinforcement range optimization method to optimize the originally designed reinforcement range and grouting thickness. As shown in Fig. 6, the optimized parameters are detailed in Table 3.

As shown in Fig. 9 (a), the ring grouting method is implemented based on the CD excavation method by applying a grouting reinforcement ring for advanced pre-grouting reinforcement. The primary approach involves pre-grouting reinforcement of the surrounding rock mass around the tunnel prior to excavation.

As shown in Fig. 9 (b), the grouting range is expanded compared to the original grouting method. The grouting range is increased from 1.5 m to 2.0 m, enhancing the overall reinforcement effectiveness.

4.1 Displacement and deformation of surrounding rock

According to the calculation results of the model, it is found that the displacement and deformation of surrounding rock at different monitoring points are different when different grouting reinforcement methods are used for excavation, as shown in Figs. 10 and 11.

Table 3 Grouting reinforcement measures

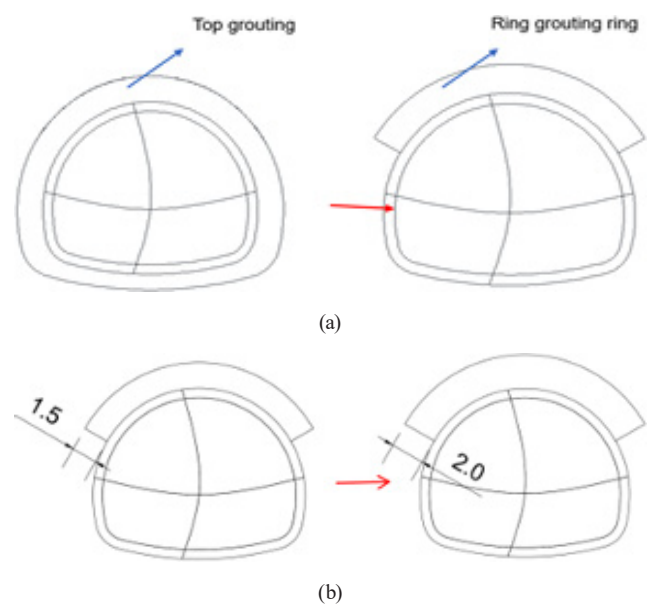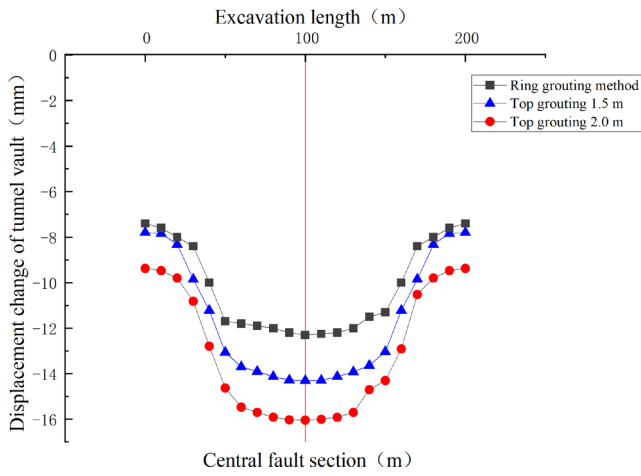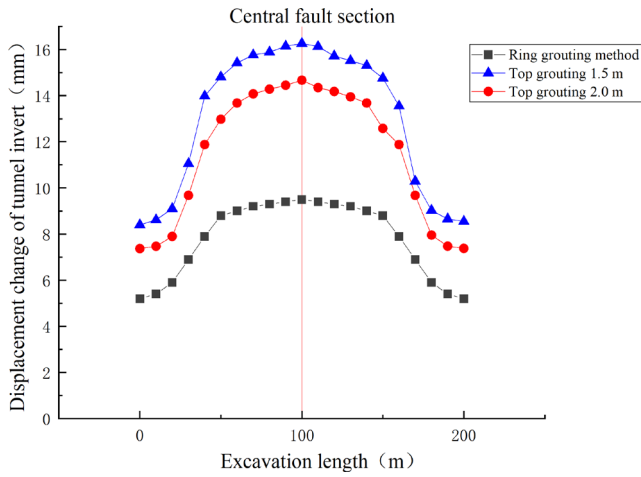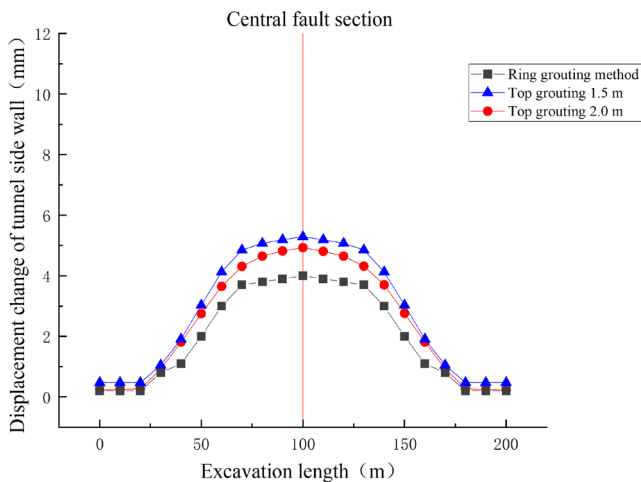| Grouting method	Grouting material	Reinforcement range (°)	Reinforcement thickness (m)
Reinforced by grouting at the top	Cement mortar	120	1.5
Ring grouting method	Cement mortar	360	1.5
Reinforcement range optimization	Cement mortar	120	2.0

(a)

(b)

Fig. 9 Optimization diagram of grouting method; (a) Optimization of reinforcement range; (b) Optimization of grouting range

Table 2 Stress distribution

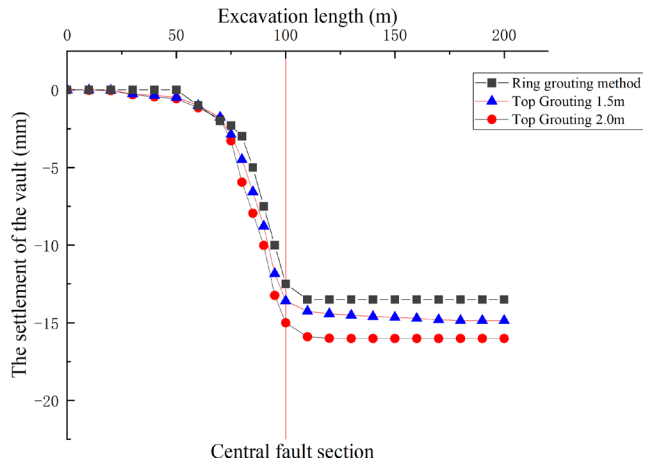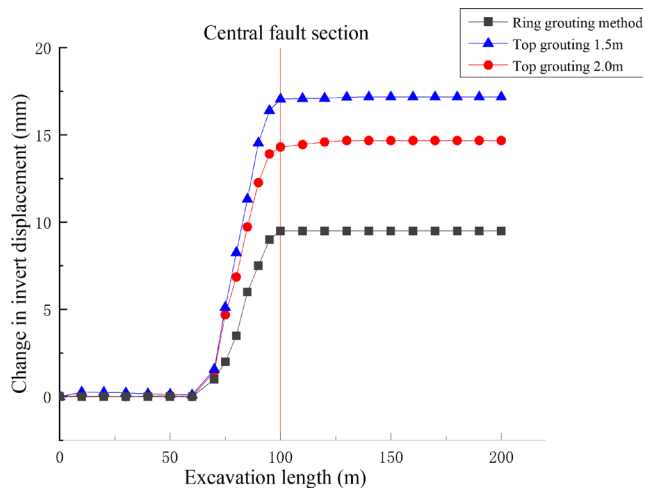| Excavation method	Maximum principal stress (MPa)	Distribution position	Minimum principal stress (MPa)	Distribution position
Reserve core soil method	0.47	Invert	−1.87	Hogging
CD method	0.77	Vault	−1.99	Corner
CRD method	0.38	Vault	−1.41	Corner

Fig. 10 The final displacement curve of the key points of the fracture zone along the excavation direction; (a) Vault; (b) Invert; (c) Side walls

Fig. 11 The displacement curve of key points in the central section of fault with excavation; (a) Vault; (b) Invert; (c) Side walls
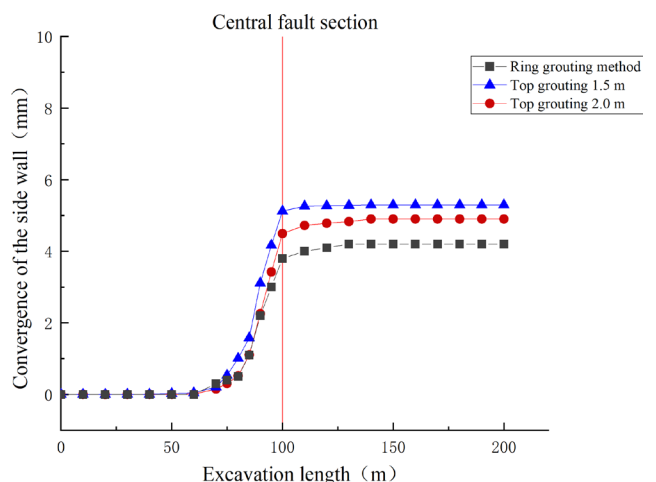
According to Fig. 10 compared with ordinary grouting method, circular grouting method has better reinforcement effect. After adopting this grouting method, it can effectively improve the stability of surrounding rock, improve the control effect of surrounding rock deformation during excavation, and reduce the overall deformation of surrounding rock during excavation.

As can be seen from Fig. 10, after the grouting range is increased, the invert uplift and side wall convergence generated by tunnel excavation decrease, but the arch roof settlement remains basically unchanged. It can be seen that the deformation of surrounding rock caused by excavation can be reduced to a certain extent by increasing the reinforcement range of grouting.

According to Fig. 11, during the excavation of the central section of the fault, tunnel excavation significantly reduces the deformation of surrounding rock generated by the central section of the fault. Thus, this grouting reinforcement method can effectively ensure the overall safety of the construction, and is recommended for the excavation of weak surrounding rock belt.

4.2 Stress distribution of supporting structure

Through comparison of model calculation results, it is found that the maximum and minimum principal stresses of 2.0 m grouting at the top and ring grouting methods are reduced, as shown in Table 4.

As shown in Table 4, the ring grouting method can improve the overall stability of surrounding rock, thereby reducing the tensile stress and compressive stress borne by the tunnel supporting structure, and keeping the stress borne by the tunnel supporting structure within the safe range. Such strengthening measures effectively improve the stability and safety of the structure.

5 Conclusions

This paper addresses the critical engineering challenges of poor surrounding rock stability and low construction safety during tunnel excavation through fault fracture zones. A comparative analysis of the deformation and stress distribution of the surrounding rock is conducted for three commonly applied excavation methods: the reserved core soil method, the CD method, and the cross CRD method. The analysis identifies the excavation method that offers the highest level of safety under these complex geological conditions. Furthermore, the study evaluates the feasibility and effectiveness of the ring grouting method and the optimization of grouting reinforcement range. Results demonstrate that optimizing the

reinforcement zone significantly enhances surrounding rock stability and minimizes construction risks, providing a robust framework for safe and efficient tunnel construction in fault zones:

1. The settlement displacement of the arch roof caused by different excavation methods follows the order: reserved core soil method > CD method > CRD method. Similarly, the uplift displacement of the invert and the convergence displacement of the sidewalls also follow the same trend: reserved core soil method > CD method > CRD method. These findings indicate that the CRD method demonstrates superior control over surrounding rock deformation when excavating through fault fracture zones. The effectiveness of the CRD method in deformation control can be attributed to its use of a central partition during excavation and its smaller excavation volume. This method significantly reduces the disturbance to the surrounding rock near the excavation face, effectively minimizing displacement during tunnel construction.

2. When different excavation methods are employed, the displacement trends of the surrounding rock at each monitoring point along the central section of the fault exhibit similar patterns. Significant displacement changes are observed at each monitoring point during the excavation of the central fault section, with a marked increase in displacement magnitude. However, the rate of displacement stabilizes and tends to level off after the initial support is completed.

3. Under different excavation methods, the tunnel supporting structure usually has a large tensile stress in the vault, while the maximum compressive stress is mainly concentrated in the side wall or corner. Before the implementation of the optimization grouting reinforcement measures, the supporting structure may be subjected to tensile stress beyond its maximum tensile strength, which may lead to the failure of the supporting structure and affect the stability of the tunnel. After ring grouting method and reinforcement area optimization method, the maximum

Table 4 Stress distribution

Excavation method	Maximum principal stress (MPa)	Distribution position	Minimum principal stress (MPa)	Distribution position
Top grouting 1.5 m	0.77	Vault	−1.99	Corner
Top grouting 2.0 m	0.75	Vault	−1.95	Corner
Ring grouting	0.45	Vault	−1.81	Corner

tensile stress and compressive stress of the supporting structure are reduced, and can be maintained within the safe range of the tensile strength and compressive strength of the supporting structure. Such strengthening measures effectively improve the stability and safety of the structure.

References

[1] Huo, S. S., Tao, Z. G., He, M. C., Xu, C., Wang, F. N., Lv, Z. Y. "Physical model test of NPR anchor cable-truss coupling support system for large deformation tunnel in fault fracture zone", Tunnelling and Underground Space Technology, 152, 105939, 2024.
https://doi.org/10.1016/j.tust.2024.105939

[2] Jiang, Q.-H., Zhang, J.-Z., Zhang, D.-M., Huang, H.-W., Shi, J.-K., Li, Z.-L. "Influence of geological uncertainty on longitudinal deformation of tunnel based on improved coupled Markov chain", Engineering Geology, 337, 107564, 2024.
https://doi.org/10.1016/j.enggeo.2024.107564

[3] Guo, Y., Wang, X., Liu, H., Liu, Y., Ma, C., Li, Z., Li, W., Li, K., Zhang, J., Chen, J. "Research on Pre-grouting Strengthening Technology of Shallow and Large Section Metro Tunnel through Fault Fracture Zone", IOP Conference Series: Earth and Environmental Science, 189, 052057, 2018.
https://doi.org/10.1088/1755-1315/189/5/052057

[4] Liu, X., Fang, H., Jiang, A., Zhang, D., Fang, Q., Lu, T., Bai, J. "Mechanical behaviours of existing tunnels due to multiple-tunnel excavations considering construction sequence", Tunnelling and Underground Space Technology, 152, 105870, 2024.
https://doi.org/10.1016/j.tust.2024.105870

[5] Tang, J., He, M., Bian, H., Qiao, Y. "A novel numerical framework to simulate mechanical response and damage characteristics of mountain tunnels under faulting", Engineering Failure Analysis, 158, 108030, 2024.
https://doi.org/10.1016/j.engfailanal.2024.108030

[6] Chen, L., Wang, Y., Wang, Z.-F., Fan, F., Liu, Y. "Characteristics and treatment measures of tunnel collapse in fault fracture zone during rainfall: A case study", Engineering Failure Analysis, 145, 107002, 2023.
https://doi.org/10.1016/j.engfailanal.2022.107002

[7] Shou, K.-J. "A three-dimensional hybrid boundary element method for non-linear analysis of a weak plane near an underground excavation", Tunnelling and Underground Space Technology, 15(2), pp. 215–226, 2000.
https://doi.org/10.1016/S0886-7798(00)00047-X

[8] Gao, J., Peng, S., Chen, G., Fan, H. "An extended discontinuous deformation analysis for simulation of grouting reinforcement in a water-rich fractured rock tunnel", Journal of Rock Mechanics and Geotechnical Engineering, 2024.
https://doi.org/10.1016/j.jrmge.2023.12.029

[9] He, M., Sui, Q., Li, M., Wang, Z., Tao, Z. "Compensation excavation method control for large deformation disaster of mountain soft rock tunnel", International Journal of Mining Science and Technology, 32(5), pp. 951–963, 2022.
https://doi.org/10.1016/j.ijmst.2022.08.004

[10] Xu, X., Wu, Z., Weng, L., Chu, Z., Liu, Q., Wang, Z. "Investigating the impacts of reinforcement range and grouting timing on grouting reinforcement effectiveness for tunnels in fault rupture zones using a numerical manifold method", Engineering Geology, 330, 107423, 2024.
https://doi.org/10.1016/j.enggeo.2024.107423

[11] Jeon, S., Kim, J., Seo, Y., Hong, C. "Effect of a fault and weak plane on the stability of a tunnel in rock—a scaled model test and numerical analysis", International Journal of Rock Mechanics and Mining Sciences, 41, pp. 658–663, 2004.
https://doi.org/10.1016/j.ijrmms.2004.03.115

[12] Ghaboussi, J., Ranken, R. E. "Interaction between two parallel tunnels", International Journal for Numerical and Analytical Methods in Geomechanics, 1(1), pp. 75–103, 1977.
https://doi.org/10.1002/nag.1610010107

[13] Ji, M., Wang, X., Luo, M., Wang, D., Tang, H., Du, M. "Stability Analysis of Tunnel Surrounding Rock When TBM Passes through Fracture Zones with Different Deterioration Levels and Dip Angles", Sustainability, 15(6), 5243, 2023.
https://doi.org/10.3390/su15065243

[14] Xue, Y., Li, G., Yang, W., Qiu, D., Su, M. "Analysis and optimization design of submarine tunnels crossing fault fracture zones based on numerical simulation", Marine Georesources & Geotechnology, 38(9), pp. 1106–1117, 2020.
https://doi.org/10.1080/1064119X.2019.1655120

[15] Li, P., Xie, S., Yang, X., Wang, Z., Wang, S. "Investigation into the Construction Response of Tunnels through Fault: Model Test", Applied Sciences, 13(7), 4460, 2023.
https://doi.org/10.3390/app13074460

[16] Chinese Standard "JTG 3660-2020 公路隧道施工技术规范" (JTG 3660-2020 Code for design of highway tunnels), Standardization Administration of the People's Republic of China, Beijing, China, 2020. (in Chinese)

[17] Chinese Standard "TB10003-2016 铁路隧道设计规范" (TB10003-2016 Code for design on tunnel of railway), China Railway Second Institute Engineering Group , Beijing, China, 2016. (in Chinese)

[18] Chinese Standard "GB50218-2014 工程岩体分级标准" (GB50218-2014 Engineering rock mass classification standard), Standardization Administration of the People's Republic of China, Beijing, China, 2014. (in Chinese)

[19] Zheng, Y., Yan, J., Su, R., Ma, S., Li, Y., Wang, X., Zheng, J., Zhu, Y., Yu, Y. "Investigation of the settlement mechanism and control measures of a super-large section tunnel in a giant karst cave using ultra-thick backfill method", Tunnelling and Underground Space Technology, 137, 104956, 2023.
https://doi.org/10.1016/j.tust.2022.104956

[20] Wu, Y., Duan, J., Xu, J., Xu, W. "Failure Mechanism and Structural Optimization of the Primary Support Structure for Expressway Tunnel in Soft Rock: A Case Study", Periodica Polytechnica Civil Engineering, 68(4), pp. 1268–1280, 2024.
https://doi.org/10.3311/PPci.36949

[21] Xin, C., Feng, W., Song, D., Huang, S., Liu, X. "Seismic damage to non-fault-crossing and fault-crossing tunnels: Comparative study of the 2008 Wenchuan earthquake (Mw 7.9) and the 2022 Menyuan earthquake (Mw 6.7)", Engineering Failure Analysis, 166, 108843, 2024.
https://doi.org/10.1016/j.engfailanal.2024.108843